Journal of Engineering and Applied Sciences 13 (Special Issue 11): 8826-8835, 2018
ISSN: 1816-949X

Time-Frequency Cross-Correlation Function Estimation in Radars with Common Aerial for Transmission and Reception of Quasicontinuous Signals

I.N. Zhukova, N.E. Bystrov, V.M. Reganov and S.D. Chebotarev
Department of Radiosystems, Novgorod State University, B. Sankt-Peterburgskaya St. 41, Velikiy Novgorod, Russian Federation

Abstract: It is critically important for modern radars to make fast and unambiguous measurements of a target's range and Doppler frequency shift. One of the promising ways is to use quasicontinuous signals in radars with special transmission and reception mode. Quasicontinuous signals have a thumbtack shape of an ambiguity function and can be used in radars with common aerial. This study presents the quasicontinuous transmission and reception mode of a pseudorandom amplitude and phase-shift keying signals in radars with common aerial. The Time-Frequency Cross-Correlation (TFCC) function of such signals is used for describing their coherent processing result. The TFCC function approximation is given taking into account the receiver path blanking during the probing signal transmission. An example of signal clutter immunity estimation is given based on TFCC function approximation and determined statistical averaging of distribution density of the total clutter power along delay and the Doppler frequency shift.

Key words: Modern radars, quasicontinuous signals, digital signal processing, ambiguity function, time-frequency cross-correlation, power

INTRODUCTION

One of the main problems in modern radars is the range and Doppler ambiguity, caused by multiple-peak shape of the probing signal's Ambiguity Function (AF). Randomization of the pulse repetition interval is one of the ways of solving the ambiguous range and Doppler frequency shift measurement. Obviously, many methods of the range and Doppler ambiguities mitigation are described in literature. Variety of methods use inter-pulse coding which exploits the different structures of each probing pulse and leads to partial mitigating of range ambiguity (Prinsen, 1973; Levanon, 2009; Milstein, 1978). Changing the inter-pulse interval from pulse to pulse (PRF jittering, staggered PRI) is the method of ambiguity elimination using several probing periods with different PRI which obviously consumes more time to measure target range and velocity than single-period measurement. This can be unacceptable within presence of high-velocity targets (Ahmadi and Mohamedpour, 2012; Thomas and Abram, 1976; Zhu *et al*., 2016; Kaveh and Cooper, 1976).

Another ambiguity elimination method includes sequential transmission of multiple PRFs in a dwell time (Xia, 1999; Rasool and Bell, 2010; Deng *et al*., 2013). This method of ambiguity elimination is similar to PRF jittering and has similar drawbacks.

We should say that the mentioned above signals propose only partial mitigation of range and Doppler ambiguity or major increase of measurement time.

Described by Gantmaher *et al*. (2005) and Bystrov *et al*. (2017) signals with pseudorandom Amplitude and Phase-Shift Keying (APSK) completely eliminate range and Doppler ambiguity. Ambiguity function of such APSK signal is thumbtack shaped and has uniform sidelobe level in time delay and Doppler frequency shift plane:

$$t \in [-T/2, T/2], F \in [-1/2t_b, 1/2t_b]$$

Where:

T = The duration of the signal and the Coherent Processing Interval (CPI)

t_b = The duration of the coded bit

The pseudorandom pulse repetition interval and duration make it possible to detect targets at distances up to $D_{max} = Tc/2$, c speed of light with velocity up to $V_{max} = \lambda/(4t_b)$, λ is the wavelength. Hence, $D_{max}.V_{max} = Nc\lambda/8$, $N = T/t_b$.

Probing APSK signal consists of Phase-Shift Keying (PSK) pulses with non-zero amplitude and pauses between them. The pulse duration varies from pulse to pulse but it is a multiple of $t_x = k_x t_b$, k_x is an integer. The pauses between the non-zero pulses are also differ from

Corresponding Author: S.D. Chebotarev, Department of Radiosystems, Novgorod State University, B. Sankt-Peterburgskaya St. 41, Velikiy Novgorod, Russian Federation

each other and a multiple of t_x. The natural envelope of the APSK signal is a random binary sequence. When the probability of PSK pulse to be transmitted is C>0.1 such signal can be called quasicontinuous signal.

The phase-shift keying law changes from pulse to pulse. The spectrum bandwidth of quasicontinuous signal is determined by the duration of the phase-shift keyed bit t_b. The value $1/t_b$ significantly exceeds the operating range of Doppler frequency shifts of return signals, reflected from moving targets, clutter and other objects in the radar coverage area. The return signals completely overlap each other in frequency domain.

When a radar uses a common aerial for transmission and reception, the radar receive path is blanked during the transmission of probing pulse by the signal that is orthogonal to the envelope of the probing quasicontinuous signal. The return signals are received only in pauses between probing signal pulses, so, part of the return signal energy is lost. Note that the return quasicontinuous signals with different delays lose different bits during the receiver path blanking. We shall call this radar working mode a quasicontinuous mode.

After blanking in receive path the return signals are coherently processed by a multichannel correlation receiver with delays $\tau_m = m \cdot t_b$, m = 1-3 and the Doppler frequency shifts $F_v = v/T$, v = 0, ±1, ±2. In the (m, v) processing channel the receiver performs cross-correlation of the blanked return signal and reference APSK signal with (m, v) time-frequency shift. The reference signal of the (m, v) processing channel is matched to the return signal with (m, v) time-frequency shift.

The delay-Doppler response is determined by the TFCC function of the APSK signal. The cross-correlation function takes into account the receiver path blanking during the probing signal transmission. This is what differs the TFCC function from the AF.

This study investigates TFCC function. The sidelobe level of TFCC function is estimated as a function of the minimum duration of $t_x = k_x t_b$ and the probability C of the PSK pulse transmission.

Problem statement: The sidelobe level of TFCC function of the blanked return signal and the reference APSK signal determines the target detection probability and the clutter immunity of the radars with quasicontinuous working mode. The TFCC function analysis should be carried out.

It is known that, the sidelobes level of the signal AF is determined by the time-bandwidth product of the signal and decreases as the duration and/or bandwidth of the signal increases. Target detection is performed in a small time-frequency shift range, compared to the duration of the quasicontinuous signal and its spectrum bandwidth. Therefore, it is critically important to know the sidelobe level in the operating range of the time-frequency shifts near the main peak of the TFCC. The TFCC function approximation can significantly simplify the estimation of the radar clutter immunity.

It is necessary to find out how the sidelobe level and shape of the TFCC function of the quasicontinuous signal vary depending on its parameters: minimum duration of $t_x = k_x t_b$ and the probability C of the PSK pulse transmission. This will allow us to specify the best probing signal parameters for the given interference.

Research questions: This study contains:

- A mathematical description of the quasicontinuous signals and its correlation processing in radars with common aerial
- The results of TFCC function approximation which takes into account the receiver path blanking during the probing signal transmission
- The analysis results of the TFCC function shape and sidelobe level, depending on the parameters of the quasicontinuous signal

Purpose of the study: The purpose of the study was to obtain the sidelobe level estimation of the TFCC function approximation of the quasicontinuous signals which takes into account the receiver path blanking during the probing signal transmission.

MATERIALS AND METHODS

The theoretical and methodological basis of the study is a set of methods, main of which is mathematical modeling of wide bandwidth signal synthesis and processing.

The basis of the study is the analysis method; synthesized signals were investigated under this method. The creation of a mathematical model for the synthesis and processing of the quasicontinuous signal allowed us to thoroughly analyze the shape and level of the side lobes of the cross-correlation function.

RESULTS AND DISCUSSION

Mathematical definition of the quasicontinuous signal and its correlation processing: Let C be the probability of the PSK pulse to be transmitted. The length of the PSK pulse is $t_x = k_x t_b$ where k_x is an integer, t_b is the duration of the coded bit. The duration of the signal can be

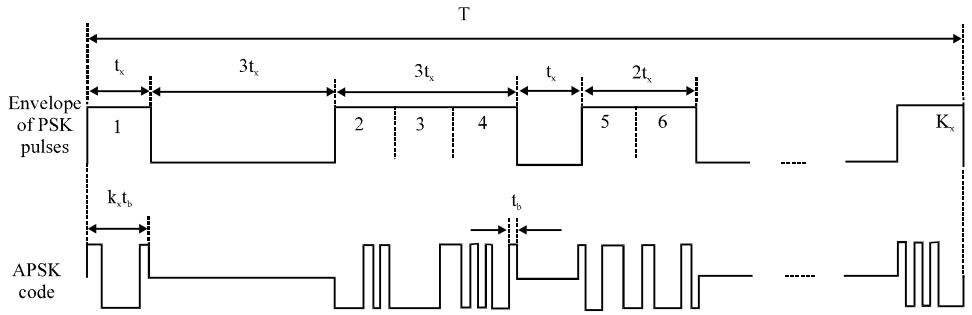

Fig. 1: The structure of the quasicontinuous signal

defined as $T = Nt_b = N_x t_x$, $N = N_x k_x$. Therefore, the number of the transmitted phase coded pulses of the length t_x is $K_x = CN_x$ and the total number of transmitted coded bits of the length t_b is $K = CN$.

Figure 1 shows the structure of the quasicontinuous signal which consists of the random train of the PSK pulses. Let the random binary sequence x_i, $x_i \in \{1, 0\}$, $i = 0, \ldots, N_x\text{-}1$, determines the phase coded pulse position along time axis 0, ..., T. The parameter $C = K_x t_x/T$ defines the average duty cycle of the PSK pulses.

The random discrete sequence φ_n, $\varphi_n \in [0, \pi]$, $n = 0, \ldots, N\text{-}1$, sets N phases $\{\varphi_0, \varphi_1, .., \varphi_{N-1}\}$. The envelope of the quasicontinuous signal is given by:

$$u(t) = \frac{1}{\sqrt{t_b}} \sum_{i=0}^{N_x-1} x_i \sum_{i_x=0}^{k_x-1} \exp\left(j\varphi_{i\times k_x+i_x}\right) \cdot \text{rect}\left[\frac{t-(i\times k_x+i_x)t_b}{t_b}\right] 0 \le t < T \quad (1)$$

The APSK code, associated with u(t) is defined by $w_{ik_x+i_x} = x_i \exp\left(j\varphi_{ik_x+i_x}\right)$, $i = 0, ..., N_x\text{-}1$, $i_x = 0, ..., k_x\text{-}1$. Each bit is assigned (or coded) with its own phase value and one of two possible amplitude values (0 or 1). Equation 1 can be represented as Eq. 2:

$$u(t) = \frac{1}{\sqrt{t_b}} \sum_{n=0}^{N-1} w_n \cdot \text{rect}\left[\frac{t-n\cdot t_b}{t_b}\right] \quad (2)$$

The modulus $|w_n|$, $n = 0, .., N\text{-}1$, determines the natural envelope of the quasicontinuous signal. The quasicontinuous signal energy can be expressed as:

$$E = \int_0^T |u(t)|^2 dt = \sum_{n=0}^{N-1} |w_n|^2 = k_x \sum_{i=0}^{N_x-1} x_i = k_x C N_x = CN = K$$

The simplest synthesis method of code sequences x_i and φ_n is to use the rnd (a) function to generate uniformly distributed random values in the range [0, a]:

$$x_i = \begin{cases} 1, & \text{rnd}(1) \le C \\ 0, & \text{rnd}(1) > C \end{cases} \quad \varphi_n = \begin{cases} 0, & \text{rnd}(1) \le 1/2 \\ \pi, & \text{rnd}(1) > 1/2 \end{cases} \quad (3)$$

For the quasicontinuous signals synthesis other sequences with the random properties can be used such as pseudorandom sequences, Gold codes, GMW-sequences (Singer, 1938; Gold, 1967; Martin and Sole, 2008). For the phase-shift keying different modulation schemes can be used including bi-phase, quadrature and multiphase.

For instance, in this study, we will describe the quasicontinuous signal with parameters: N = 1248, C = 0.2 and $k_x = 8$. The sequence x_i is a pseudorandom binary sequence. It has the length $N_x = 156$. The sequence φ_n is synthesized using the rnd function. Such short signal length is not usual for a radar, we use it just for convenient presentation of signal's structure at Fig. 2a, b. For real radar purposes, it is possible to synthesize quasicontinuous signal with length up to several hundred thousand bits.

In radars with common aerial for transmission and reception the correlation processing of return signal is given by:

$$\left|X(\tau_m, F_v)\right| = \left|\int_0^T u_R(t) u_{Blank}(t) u^*(t-\tau_m) \exp(-j2\pi F_v t) dt\right| \quad (4)$$

where, $u_R(t)$ the processed signal which represents a linear sum of the return signals with the different delays and Doppler frequency shifts and clutter:

$$u_{Blank}(t) = \sum_{i=0}^{N_x-1} (1-x_i) \cdot \text{rect}\left(\frac{t-i\cdot t_x}{t_x}\right)$$

is the blanking signal for receiver path; $\tau_m = m\cdot t_b$, $m = 1, 2, 3, ...$, is the delay shift and $F_v = v/T$, $1 = 0, \pm 1, \pm 2, \ldots$, is the Doppler frequency shift of the multichannel correlation receiver; *the complex conjugation sign.

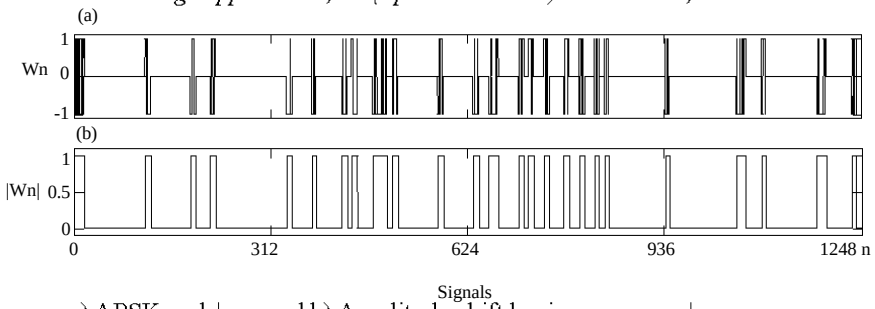

Fig. 2: Signal diagrams: a) APSK code|. w_n and b) Amplitude-shift keying sequence $|w_n$

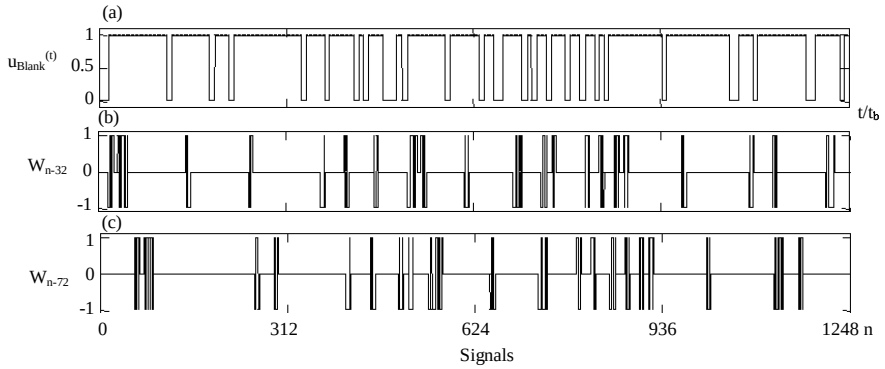

Fig. 3: Signal diagrams: a) The blanking signal; b) The return signal envelope with time shift $32t_b$ and c) The return signal envelope with time shift $72t_b$

When the $x_i = 1$ the signal $u_{Blank}(t) = 0$, $t = i \cdot t_x$ and the receiver path is blanked. If at this time the return processed signal $u_R(t)$ contains the nonzero coded pulse of the signal with the delay τ_m and Doppler frequency shift F_v, then this pulse will be rejected and lost.

When the $x_i = 0$ the signal $u_{Blank}(t) = 1$, $t = i \cdot t_x$. These moments are the pauses in the transmission and the radar receives the return signals. The return signal pulse with the delay τ_m and Doppler frequency shift F_v will be accumulated in (m, v)-th processing channel.

The blanking signal $u_{Blank}(t)$ has only two values 0 and 1. It simultaneously blanks the processing signal $u_R(t)$ and the reference signals with different delays τ_m. Thus, we may say that the processing of the quasicontinuous signal with the delay τ_m in the m-th processing channel remains matched.

The return signals with different delays lose different bits when the receiver is blanked. We can see it comparing Fig. 2 and 3. Figure 3a depicts the blanking signal for the signal from Fig. 2. Figure 3b, c show two return signals with different delays after blanking at the receiver path.

The time-frequency cross-correlation function and its approximation: The function $|X(\tau_m, F_v)|$ is the time-frequency response of the multichannel correlation receiver of the quasicontinuous signals.

Let the signal $u_R(t)$ be the pinpoint target with unit amplitude, delay $\tau_S = s \cdot t_b$, s = 1,2, ... and Doppler frequency shift $F_S = v_S/T$, $v_S = 0,\pm1,...$ Then the multichannel correlation receiver response (Eq. 4) to the signal $u_R(t) = u(t-\tau_S) \exp(j2\pi F_S t)$ can be written as:

$$\left|X(\tau_m, F_v)\right| = \left|\int_0^T u(t-\tau_S)u_{Blank}(t)u^* (t-\tau_m)\exp\left[j2\pi(F_S-F_v)t\right]dt\right| \quad (5)$$

Let us denote $\tau = \tau_S - \tau_m$, $F = F_S - F_v$ by the time and Doppler frequency shift mismatch, respectively. We can get Eq. 6 which represents the TFCC function of the $[u(t-\tau_S)u_{Blank}(t)]$ and the reference signal of (m,v)-th processing channel by the variable change in Eq. 5:

$$\left|\chi_{\tau_S}(\tau, F)\right| = \left|\int_0^T u(t)u_{Blank}(t+\tau_S)u^*(t+\tau)\exp\left[j2\pi Ft\right]dt\right| \quad (6)$$

Equation 6 differs from the AF of APSK signal by an additional multiplier $u_{Blank}(t)$ which represents the receiver path blanking.

Value $|\chi_{\tau s}(0, 0)|$ represents the energy of the APSK signal with unit amplitude after blanking. When $\tau \neq 0$ and/or $F \neq 0$, the value $|\chi_{\tau s}(\tau, F)|$ determines the interference in m, v-th processing channel from the signal with delay $\tau_S \neq \tau_m$ and Doppler frequency shift $F_S \neq F_v$.

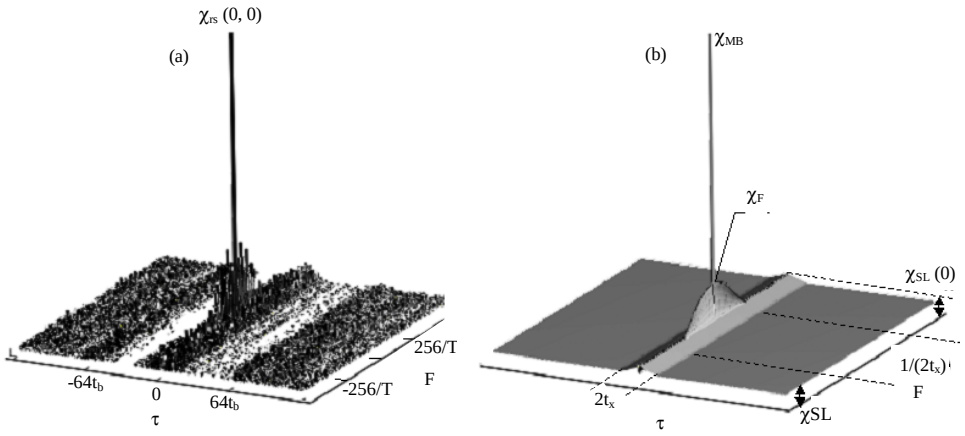

Fig. 4: a) The TFCC function and b) The TFCC function approximation

Mathematical modeling showed, that the shape of TFCC function $|\chi_{\tau s}(\tau, F)|$ is slightly depends on the delay τ_S and is determined only by the mismatch in the delay τ and the Doppler frequency shift F. Figure 4a shows the typical TFCC function.

TFCC function of quasicontinuous signal is thumbtack shaped and has uniform sidelobe level in time delay and Doppler frequency shift plane: $\tau\in[-T/2,-t_x]\cup[t_x, T/2]$, $F\in[-1/2t_b, 1/2t_b]$. In the delay range $\tau\in[-t_x, t_x]$ there is a "Comb" with an increased level of sidelobes. The length of the "Comb" along the frequency axis is $F\in[-1/2t_b, 1/2t_b]$. We should mention that sidelobes level also increase near the main peak of TFCC function when $\tau = 0$. We propose the TFCC function approximation that is shown in Fig. 4b.

Estimation of the main peak and the sidelobes level of the TFCC function: The magnitude of the TFCC function main peak $|\chi_{\tau s}(\tau, F)|$ is defined by Eq. 7:

$$\left|\chi_{\tau_S}(0, 0)\right| = \left|\int_0^T u_{blank}(t+\tau_S)\left|u(t)\right|^2 dt\right| \quad (7)$$

In Eq. 7, the signal delay $\tau_s = \tau_m+\tau' = m\cdot t_b+\tau'$, m = 0,1,2, ..., $0<\tau'\le t_b$. The quasicontinuous signal consists of the coded pulses of duration $t_x = k_x t_b$. Therefore, the signal delay can be written as $\tau_s = (m_x k_x+i_x)\cdot t_b+\tau'$, $m_x = 0, 1, 2, .., i_x = 0, 1, ..., (k_x-1)$. Taking this into account, expression Eq. 7 is transformed to Eq. 8:

$$\left|\chi_{\tau_S}(0,0)\right| = \left[\sum_{n=0}^{N-1}\left(1-\left|w_{n-m}\right|\right)\left|w_n\right|\right]\psi(\tau', 0) = \left[K-i_x\sum_{i=0}^{N_x-1}x_{i-m_x+1}x_i-\left(k_x-i_x\right)\sum_{i=0}^{N_x-1}x_{i-m_x}x_i\right]\psi(\tau',0) \quad (8)$$

Where:

$$\psi(\tau', F) = \frac{1}{t_b}\int_0^{t_b}\text{rect}\left(\frac{t}{t_b}\right)\text{rect}\left(\frac{t+\tau'}{t_b}\right)\exp(j2\pi Ft)dt$$

is the AF of the single bit. Figure 5 shows $|\chi_{\tau s}(0, 0)|/E$ for different τ_S of two signals with following parameters: N = 4096, C = 0.2, k_x = 16 (Fig. 1); N = 16384, C = 0.5, k_x = 64 (Fig. 2). The values N and k_x of these signals differ by a factor of 4. The curves depict the change in energy of return signal $|\chi_{\tau s}(0, 0)|$ after the blanking in receiver path against its varying delay.

Note that the energy of the blanked signal $|\chi_{\tau s}(0, 0)|$ linearly increases with a change of the delay in the range $(\tau_S/t_b) = 1, ..., k_x$. For delays $(\tau_S/t_b)>k_x$ there is a values scatter of $|\chi_{\tau s}(0, 0)|$ relative to the constant level. The mean of $|\chi_{\tau s}(0, 0)|$ is defined as:

$$\chi_{MB} = \frac{1}{T}\int_0^T\left|\chi_{\tau_S}(0, 0)\right|d\tau_S = \frac{1}{N}\sum_{m=0}^{N-1}\left[K-\sum_{n=0}^{N-1}\left|w_{n-m}\right|\left|w_n\right|\right] = NC(1-C) = NC_P \quad (9)$$

In Eq. 9, the subtrahend in square brackets stands for the number of blanked pulses. Energy loss in the quasicontinuous working mode is determined by the Autocorrelation Function (ACF) of the APSK signal envelope. The value of χ_{MB} of the TFCC function depends only on the probability C of the PSK pulse to be transmitted and is determined by the probability value $C_P = C(1-C)$. The C_P is the probability of return signal coded pulse to pass the receiver blanking and to be received and accumulated.

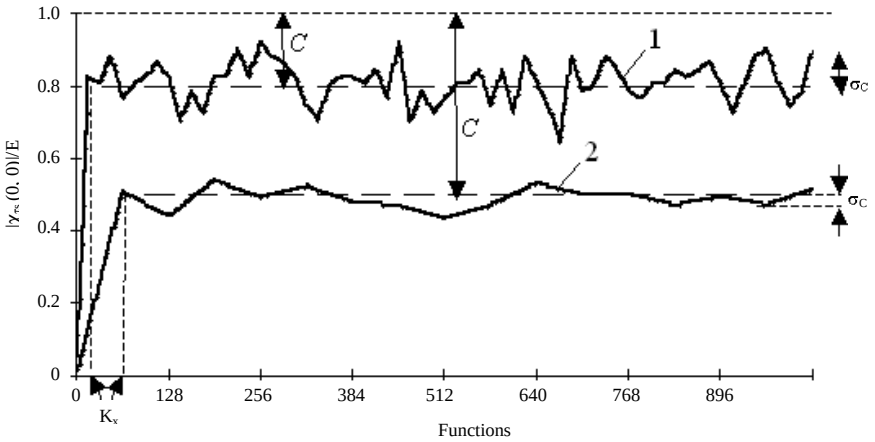

Fig. 5: Normalized energy of TFCC function peak

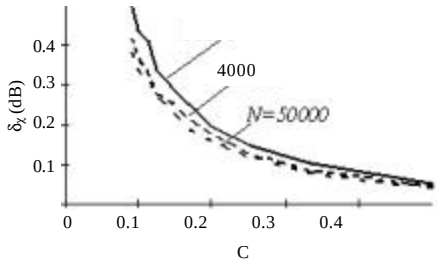

Fig. 6: The deviation of the χ_{MB}

The graphs, outlined in Fig. 5 have the following values of χ_{MB}: $\chi_{MB}/E = 0.8$ for $C = 0.2$ and $\chi_{MB}/E = 0.5$ for $C = 0.5$. This means that for the probability of pulse transmission $C = 0.5$ half of the return signal energy is lost and for $C = 0.2$ one fifth of the return signal energy.

The $|\chi_{\tau s}(0, 0)|$ values scatter relative to the mean level of $\chi_{1\hat{A}}$ depends on the probability C and the length $N_x = N/k_x$. Figure 6 shows the variation graphs of the ratio $\delta_\chi = |\chi_{MB}-\sigma_\chi|/\chi_{1\hat{A}}$ where σ_χ is the RMS deviation $|\chi_{\tau s}(0, 0)|$ from the χ_{MB}.

The shape of the $|\chi_{\tau s}(\tau, F)|$ function along the Doppler frequency shift axis is defined by the amplitude spectrum shape of envelope $u_{Blank}(t+\tau_s)|u(t)|^2$:

$$\chi_{\tau_S}(0, F) = \int_0^T u_{Blank}(t+\tau_S)\left|u(t)\right|^2 \exp(j2\pi Ft)dt \qquad (10)$$

$|\chi_{\tau s}(0, F)|^2$ is the Fourier transform of the autocorrelation function of the blanked signal envelope $u_{Blank}(t+\tau_s)|u(t)|^2$:

$$\left|\chi_{\tau_S}(0, F)\right|^2 = \int_0^T R_{\tau s}(\tau)\exp(-j2\pi F\tau)d\tau \qquad (11)$$

Where:

$$R_{\tau s}(\tau) = \int_{-\infty}^{\infty} u_{Blank}(t+\tau_S)\left|u(t)\right|^2 u_{Blank}(t+\tau_S+\tau)\left|u(t+\tau)\right|^2 dt$$

Since, the C_P is the probability that the instantaneous value $u_{Blank}(t+\tau_s)|u(t)|^2 \neq 0$, the value C_P^2 is the probability that the instantaneous value $[u_{Blank}(t+\tau_s)|u(t)|^2 u_{Blank}(t+\tau_s+\tau)|u(t+\tau)|^2] \neq 0$. As already highlighted, the C_P is the probability of quasicontinuous signal coded pulse to be processed. The averaged over τ_S ACF $R_{\tau s}(\tau)$ can be expressed as:

$$\overline{R_{\tau s}(\tau)} = \begin{cases} \frac{N}{t_b}C_P(1-C_P)\left(1-\frac{|\tau|}{t_x}\right)+\frac{N}{t_b}C_P^2 & |\tau| \le t_x \\ \frac{N}{t_b}C_P^2 & t_x < |\tau| \le T/2 \end{cases} \qquad (12)$$

We can express (Eq. 11) as:

$$\left|\chi_{\tau_S}(0,F)\right|^2 = \frac{NC_P(1-C_P)}{t_b}\int_{-t_x}^{t_x}\left(1-\frac{|\tau|}{t_x}\right)\exp(-j2\pi F\tau)d\tau + \frac{NC_P^2}{t_b}\int_{-T/2}^{T/2}\exp(-j2\pi F\tau)d\tau \qquad (13)$$

On rearrangement (Eq. 13) can be formulated as:

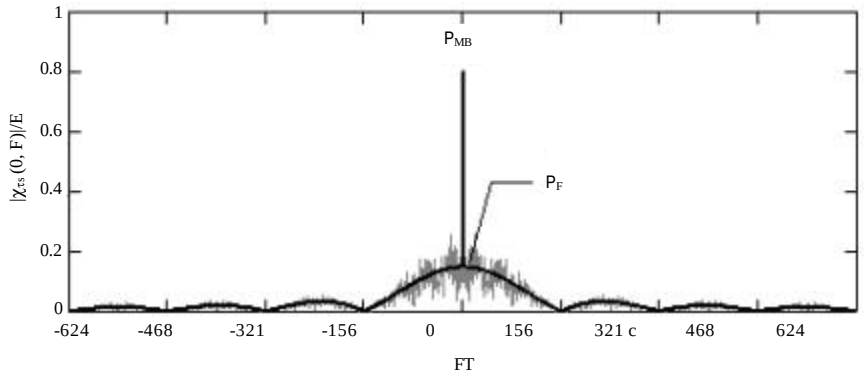

Fig. 7: The shape of the normalized TFCC function delay section and its approximation

$$|\chi_{\tau s}(0, F)|^2 = k_x NC_P(1\text{-}C_P)\left(\frac{\sin(\pi Ft_x)}{\pi Ft_x}\right)^2 + N^2C_P{}^2\frac{\sin(2\pi FT)}{2\pi FT} \quad (14)$$

We can neglect the first item of the sum (Eq. 114) due to its smallness when F = 0, so, the main peak of TFCC function equals $\chi_{MB} = NC_P$. When F≠0 the Doppler frequency shift axis becomes sinc-shaped.

An interesting case occurs when the working range of the Doppler frequency shifts is in limits F∈[-1/2t_x, 1/2t_x]. The cross interference from two return signals with the same time delay and the Doppler frequency difference |F|<1/2t_x are approximately determined by the level $\chi_F = [k_x NC_P(1\text{-}C_P)]^{1/2}$.

The $|\chi_{\tau s}(0, F)|/E$ for the signal with parameters: N = 1248, C = 0.2 and k_x = 8 and its approximation are shown in Fig. 7. The Integrated Side Lobe Ratio (ISLR) of the TFCC function when τ = 0 is defined by:

$$ISLR_{\tau=0} = 10\log_{10}\left(\frac{\int_{-1/2t_b}^{1/2t_b}|\chi_{\tau s}(0, F)|^2\,dF - \int_{-1/2T}^{1/2T}|\chi_{\tau s}(0, F)|^2\,dF}{\int_{-1/2T}^{1/2T}|\chi_{\tau s}(0,F)|^2\,dF}\right) = 10\cdot\log\left(\frac{1\text{-}C_P}{C_P}\right) \quad (15)$$

In Eq. 15 sidelobe energy equals to:

$$k_x NC_P(1\text{-}C_P)\int_{-1/2t_b}^{1/2t_b}\left(\frac{\sin(\pi Ft_x)}{\pi Ft_x}\right)^2 dF = \frac{N^2C_P(1\text{-}C_P)}{T}$$

energy in the mainlobe equals to:

$$\int_{-1/2T}^{1/2T}|\chi_{\tau s}(0, F)|^2\,dF = \frac{N^2C_P{}^2}{T}$$

When, τ≠0 the sidelobes are distributed relative to the RMS level:

$$\chi_{SL}{}^2(\tau) = t_b\int_{-1/(2t_b)}^{1/(2t_b)}|\chi_{\tau s}(\tau, F)|^2\,dF = \begin{cases} N?_{?}(1\text{-}C)\left(1\text{-}\frac{|\tau|}{t_x}\right)+N?_{?}? & 0<|\tau|\le t_x \\ N?_{?}? & t_x<|\tau|\le T/2 \end{cases} \quad (16)$$

In the range 0<|τ|<t_x the TFCC function has the "comb" with an increased sidelobes level. The "comb" has a triangular shape along the time axis, its width is 2t_x and it lies along the frequency axis. Outside the "comb", the TFCC function values change near the constant level $\chi_{SL}{}^2 = NC_PC$. The ISLR in time delay and Doppler frequency shift plane (τ∈[-T/2, T/2], F∈[-1/2t_b, 1/2t_b]):

$$ISLR = 10\log_{10}\left(\frac{\text{Total energy of the sidelobes}}{\text{Energy of the main peak}}\right) = 10\log_{10}\left(\frac{\int_0^T\int_{-1/2t_b}^{1/2t_b}|\chi_{\tau s}(\tau, F)|^2\,dFd\tau - \int_{-t_b/2}^{t_b/2}\int_{-1/2t_b}^{1/2t_b}|\chi_{\tau s}(\tau, F)|^2\,dFd\tau}{\int_{-t_b/2}^{t_b/2}\int_{-1/2t_b}^{1/2t_b}|\chi_{\tau s}(\tau, F)|^2\,dFd\tau}\right) \quad (17)$$

In Eq. 17:

$$\int_0^T\int_{-1/2t_b}^{1/2t_b}|\chi_{\tau_S}(\tau, F)|^2\,dFd\tau = \frac{1}{t_b}\int_0^T\int_0^T|u(t)|^2|u_{Blank}(t+\tau_S)|^2|u^*(t+\tau)|^2\,dtd\tau = \frac{N^3CC_P}{T})$$

$$\int_{-t_b/2}^{t_b/2}\int_{-1/2t_b}^{1/2t_b}|\chi_{\tau s}(\tau, F)|^2\,dFd\tau = \frac{N^2?_P{}^2}{T}$$

Then, Eq. 17 transforms to ISLR = 10 $\log_{10}$(N/1-C-1). ISLR increases 1/(1-C) times.

Quasicontinuous signal clutter immunity estimation based on its TFCC function approximation: Obtained value estimates of the main peak χ_{MB} and sidelobes χ_{SL} allow us to analyze the clutter immunity of the quasicontinuous signals. Let the received signal $u_R(t)$ = [s(t)+ξ(t)+η(t)] be the linear sum of three signals:

The valid signal $s(t) = A_s u(t-\tau_s)\exp(j2\pi v_s t+\varphi_s)$ with amplitude A_s, delay τ_s, Doppler frequency shift v_s and random initial phase φ_s. The clutter, that is formed by the targets in the radar's coverage area:

$$\xi(t) = \int_{-\infty}^{\infty}\int_{0}^{\infty} \rho(\tau_\xi, v_\xi)\cdot u(t-\tau_\xi)\cdot \exp(j2\pi v_\xi t)\,d\tau_\xi dv_\xi \quad (18)$$

where, the statistical averaging $|\rho(\tau_\xi,F_\xi)|^2$ determines the distribution density of the total interference power along delay τ_ξ and the Doppler frequency shift F_ξ.

The clutter η(t) with the normal distribution law and power P_0 in the signal band. Clutter immunity of quasicontinuous signals is estimated as the Signal-to-Clutter-plus-Noise Ratio (SCNR) after correlation processing:

$$q^2(\tau_S, F_s) = \frac{|A_S|^2\cdot \chi_{MB}^2}{P_{Noise}+P_{Clutter}} \quad (19)$$

Where:

$$P_{Noise} = P_0\cdot\chi_{MB} P_{Clutter} = \int_{-\infty}^{\infty}\int_{0}^{\infty}\left|\rho(\tau_\xi, F_\xi)\right|^2 \left|\chi_{\tau s}(\tau_S-\tau_\xi, F_S-F_\xi)\right|^2 d\tau_\xi dF_\xi$$

Suppose that interference is given in a limited range of delays $\tau\in[0, \tau_{max}]$ and Doppler frequency shifts $F\in[F_{min}, F_{max}]$. For large duration T, large signal spectrum bandwidth and short duration of PSK pulses t_x the following expressions are valid: $\tau_{max}<T$ and $[F_{min}, F_{max}]<1/2t_x$. Let us assess the clutter immunity of quasicontinuous signals.

In Eq. 18, $P_{Clutter}$ is the convolution of the $|\rho(\tau_\xi,F_\xi)|^2$ and the TFCC function. Its calculation can be replaced by the sum:

$$P_{\gamma out} = P_{MB}+P_F+P_{SL} \quad (20)$$

where, $P_{BM} = \rho(\tau_s, F_s)\chi_{BM}^2$ is the interference with delay and Doppler frequency shift of the target signal, $\tau_\xi = \tau_S, F_\xi = F_S$, $P_F = (\rho_\Sigma(\tau_s)-\rho(\tau_s, F_s))\chi^2$ is the interference with $\tau_\xi = \tau_S$ and $F_\xi\neq F_S$:

$$P_{SL} = \int_{\substack{0\\ \tau_\xi\neq\tau_S}}^{\tau_{max}} \rho_\Sigma(\tau_\xi)\chi_{SL}^2(\tau_S-\tau_\xi)\,d\tau_\xi$$

is the interference with $\tau_\xi\neq\tau_S$ **И** $F_\xi\neq F_S$:

$$\rho_\Sigma(\tau_\xi) = \int_{F_{min}}^{F_{max}} \left|\rho(\tau_\xi, F_\xi)\right|^2 dF_\xi$$

Taking into account the constant sidelobes level outside the "comb" of the TFCC function, the calculation of the P_{SL} in Eq. 19 can be replaced by Eq. 20:

$$P_{SL} = \chi_{SL}^2\left(\int_{0}^{\tau_S-k_x t_b}\rho_\Sigma(\tau_\xi)\,d\tau_\xi + k_x \int_{\tau_S+k_x t_b}^{\tau_S-k_x t_b}\rho_\Sigma(\tau_\xi)\,d\tau_\xi + \int_{\tau_S+k_x t_b}^{\tau max}\rho_\Sigma(\tau_\xi)\,d\tau_\xi\right) \quad (21)$$

We cite an example of the SCNR estimation. Let us use the sequence w_n of length N = 32768, k_x = 8, C = 0.14 for the generation of the pinpoint target return signal and the interference signal in the $u_R(t)$. Suppose that clutter distribution is defined by the $|\rho(\tau_\xi,F_\xi)|$ from Fig. 8a, b:

$$P_\xi = \int_{-\infty}^{\infty}\int_{0}^{\infty}\left|\rho(\tau_\xi, F_\gamma)\right|^2 d\tau_\xi dF_\xi = 1$$

The same figure shows a pinpoint target with the power $|A_s|^2$, $|A_s|^2/P_\xi$= -25 dB. In the signal $u_R(t)$ the clutter power is higher than the noise power, P_ξ/P_0 = 34 dB. Figure 8b shows the response function of $|R(\tau_n,F_v)|$ to the signal $u_R(t)$. For N = 32768, k_x = 8, C = 0.14, we have χ_{MB}^2 = 72 dB, χ_{SL}^2 = 27.4 dB, χ_F^2 = 44.5 dB.

Calculations according to Eq. 18-20 gave and estimate of SCNR q^2 = 17 dB for the pinpoint target return signal with the delay and the Doppler frequency shift from the low-intensity noise range (Fig. 8a). At the same time, noise level is low and does not affect the value q^2. $|A_s|^2\chi_{MB}^2$ = 47 dB, P_{noise} = 17 dB, P_{MB} = -71 dB, P_{SL} = 27.4 dB, P_F = -1.7 dB.

As a result, the value q^2 is defined by the sidelobes of the TFCC function and $P_{noise}+P_{Clutter}$ = 30 dB. When the delay of the return signal from target coincides with the high-power interference signal but differs by the Doppler frequency shift, then P_F and P_{SL} increase and q^2 decreases by 2 dB. When $P_0 = P_\xi$, q^2 decreases by 3 dB.

The interference immunity is achieved by increasing the time-bandwidth product $N = T/t_b$ of the APSK signal. Increasing the peak power of the probing signal leads to

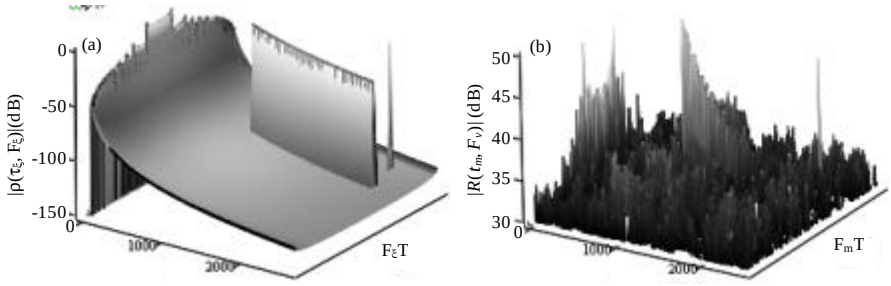

Fig. 8: The processing device output for the: a) Clutter distribution and b) Response function of simulated return signal

the $P_ξ/P_0$ and $|A_s|^2/P_0$ increase, however, $|A|^2_ξ/P_ξ$ remains unchanged. Therefore, q^2 also does not change. Methods of the sidelobe minimizing of the TFCC function are needed. One of the proposed methods is to use the APSK signals with reduced level of the sidelobes in limited range of delays and Doppler frequency shifts near the main peak of the TFCC function. This is the subject of the further research.

CONCLUSION

In this study, we analyzed the quasicontinuous signals characteristics. This analysis helps to adjust the parameters of the probing quasicontinuous signals for the specific clutter background, radar platform (marine, airborne, ground-based) and radar parameters.

The results of this research makes it possible to implement derived characteristics to mathematical model to use it in future investigations. The next step of the quasicontinuous signals research is finding the methods of minimizing the TFCC function sidelobe level. Main results are:

The approximation of the TFCC function of the APSK signals is proposed. The sidelobes level of the TFCC function is estimated depending the parameters of the APSK signal. The estimation takes into account the receiver path blanking during the pulse transmission. The examples of the sidelobes level estimation are given.

The method of radar interference immunity estimate is shown. This method uses the estimates of the sidelobes level of the TFCC function and can be applied to the radars with quasicontinuous transmission and reception of the APSK signals.

ACKNOWLEDGEMENT

The research was supported by Russian Ministry of Education, Project No. 1 8.7367.2017/8.9.

REFERENCES

Ahmadi, M. and K. Mohamedpour, 2012. PRl modulation type recognition using level clustering and autocorrelation. Am. J. Signal Process., 2: 83-91.

Bystrov, N.E., I.N. Zhukova, V.M. Reganov and S.D. Chebotarev, 2017. Range and doppler ambiguity elimination in coherent radar using quasicontinuous signals. J. Mech. Eng. Res. Dev., 40: 37-46.

Deng, Z., L. Ye, M. Fu and C. Zhao, 2013. Doppler ambiguity resolution based on random sparse probing pulses. Proceedings of the IET International Conference on Radar, April 14-16, 2013, IET, Xi'an, China, ISBN:978-1-84919-603-1, pp: 1-5.

Gantmaher, V.E., N.E. Bystrov and D.V. Chebotarev, 2005. Shumopodobnye Signaly. Nauka Publisher, Saint Petersburg, Russia,.

Gold, R., 1967. Optimal binary sequences for spread spectrum multiplexing (corresp.). IEEE. Trans. Inf. Theory, 13: 619-621.

Kaveh, M. and G.R. Cooper, 1976. Average ambiguity function for a randomly staggered pulse sequence. IEEE. Trans. Aerosp. Electron. Syst., 12: 410-413.

Levanon, N., 2009. Mitigating range ambiguity in high PRF radar using inter-pulse binary coding. IEEE. Trans. Aerosp. Electron. Syst., 45: 687-697.

Martin, B. and P. Sole, 2008. Pseudo-random sequences generated by cellular automata. Proceedings of the International Conference on Relations, Orders and Graphs: Interactions with Computer Science, May 12-17, 2008, Nouha Editions, Mahdia, Tunisie, pp: 401-410.

Milstein, L.B., 1978. Reduction of eclipsing loss in high PRF radars. IEEE. Trans. Aerosp. Electron. Syst., 14: 410-415.

Prinsen, P.J., 1973. Elimination of blind velocities of MTI radar by modulating the interpulse period. IEEE. Trans. Aerosp. Electron. Syst., 9: 714-724.

Rasool, S.B. and M.R. Bell, 2010. Efficient pulse-doppler processing and ambiguity functions of nonuniform coherent pulse trains. Proceedings of the IEEE International Conference on Radar, May 10-14, 2010, IEEE, Washington, DC, USA., ISBN:978-1-4244-5811-0, pp: 1150-1155.

Singer, J., 1938. A theorem in finite projective geometry and some applications to number theory. Trans. Am. Math. Soc., 43: 377-385.

Thomas, H.W. and T.M. Abram, 1976. Stagger period selection for moving-target radars. Inst. Electr. Eng., 123: 195-199.

Xia, X.G., 1999. Doppler ambiguity resolution using optimal multiple pulse repetition frequencies. IEEE. Trans. Aerosp. Electron. Syst., 35: 371-379.

Zhu, J., T. Zhao, T. Huang and D. Zhang, 2016. Analysis of random pulse repetition interval radar. Proceedings of the International IEEE Conference on Radar (RadarCon), May 2-6, 2016, IEEE, Philadelphia, Pennsylvania, USA., ISBN:978-1-5090-0863-6, pp: 1-5.